

Title

## Textural and chemical features of sphalerite from the Palai-Islica deposit (SE Spain): implications from colour to ore genesis

Authors

**Javier Carrillo-Rosúa, Salvador Morales-Ruano and Purificación Fenoll Hach-Alí**

**Abstract:** Sphalerite in the Au-Cu volcanic-hosted, Palai-Islica deposit appears in three locations with differences in chemistry, mainly in the Fe content: a) included in pyrite (Fe: 0.49 – 5.47 at. %) within the quartz veins; b) disseminated or in crustiform bands, also within the quartz veins; and c) disseminated in hydrothermally altered volcanic rocks from the deepest part of the deposit (Fe: 0.28 – 1.12 at. % - the only one which is cathodoluminescent). Disseminated- or crustiform band-sphalerite is the most abundant type, with two varieties: dark (Fe: 3.16 – 8.66 at. %) and light (Fe: 0.08 – 2.52 at. %). The former is associated with zones rich in gold and other metals. The Fe content of sphalerite reflects an evolution in  $f_{S_2}$  of the hydrothermal fluids. Fe-rich, “dark” sphalerite could be related to a mixing process triggering noble- and base-metal sulphide precipitation. Different types of sphalerite have significant amounts of minor elements, such as Cu (up to 1.34 at. %), Sb (up to 0.67 at. %), Sn (up to 0.31 at. %), Ge (up to 0.29 at. %), Cd (up to 0.24 at. %), In (up to 0.18 at. %), Mn (up to 0.15 at. %) and Ga (up to 0.12 at. %), some of which are elements not traditionally recognized in sphalerite. Among them, Sb, Sn, Ga-Ge and In are proportional to Cu content, and the following coupling substitutions have been demonstrated:  $Sb^{3+} + Cu^+ + Cu^{2+} \rightarrow 3Zn^{2+}$ ;  $Sn^{4+} + 2Cu^+ \rightarrow 3Zn^{2+}$ ;  $2Ge^{2+} + 1Ga^{3+} + 2Cu^{2+} + 1Cu^+ \rightarrow 6Zn^{2+}$ . The first two substitutions have been shown to produce red colouration in Fe-poor sphalerite. The latter

substitution, could be related to incorporation into the hydrothermal system of Ga-Ge bearing fluids from the basin. The presence of cathodoluminescent sphalerite seems interesting since it could reflect distinctive trace element content, and could help to distinguish a different type of mineralization and fluid/metal source manifested in an unexplored part of the deposit.

Key words: Sphalerite, epithermal deposit, Spain, Sb, Sn, colour, chalcopyrite disease, Cathodoluminescence

## **Introduction**

Sphalerite is one of the most common sulphide minerals in the earth's crust. It is not only the main zinc ore, but also associated to this mineral we find other interesting, meagre elements with high-technology applications, such as gallium, germanium and indium. It is present in highly different environments, being very common in hydrothermal systems (RAMDOHR 1969). In addition, it is suitable for a broad range of different studies which help to understand ore and rock genesis: morphological, mineral chemistry, fluid inclusion and stable isotope studies (e.g. BARTON & BETHKE 1987, BEAUDOIN 2000, BONEV & KOUZMANOV 2002, BAWDEN et al. 2003, HARMS & HECKMANN 2004; GOTTESMANN & KAMPE, 2007), and recently even for dating purposes (QIU & JIANG 2007). Sphalerite displays substantial texture diversity. For example, chalcopyrite "disease" in sphalerite has attracted a great deal of interest from different researchers (e.g. BARTON & BETHKE 1987, ELDRIGE et al. 1988, BORTNIKOV et al. 1991, BENTE & DOERING 1993, NAGASE & KOJIMA 1997). Its colouration is also extraordinarily variable (colourless, yellow, red, brown, green...) with colour marking bands and complex zonation. This colouration is mainly connected to the incorporation of different elements, especially Fe (e.g. BARTON & BETHKE 1987, RAGER et al. 1996). Thus, the chemical composition of sphalerite can be considerably complex. In addition to Zn and Fe, it hosts a

great variety of elements in minor proportions: Cu, Cd, In, Ga, Ge, Hg, Mn, Sn, Sb, Ag, Co...(e.g. OEN et al. 1980, VIETS et al. 1992, KUHLEMANN et al. 1995, ZAW & LARGE 1996, WAGNER & COOK 1998, BEAUDOIN 2000, PALERO-FERNÁNDEZ & IZARD 2005, ONO et al. 2004, GRAMMATIKOPOULOS et al. 2006).

The epithermal volcanic hosted deposit of Palai-Islica is within the Cabo de Gata-Cartagena volcanic belt in southeastern Spain, an area with a mining history that dates back to 2000 BC. This deposit, with gold and copper potential (MORALES-RUANO et al. 2000), contains abundant sphalerite distributed in different textural associations and paragenetic positions. The present study aims to characterize the textures and chemistry of sphalerite and look for their crystallochemical and geochemical implications. We specially focus on the chemical evolution of the gold-bearing system and the incorporation in sphalerite of certain elements such as Cu, Sb, Ga, Ge, Sn or In, some of which are scarce in nature. We correlate minor element composition with sphalerite colour, this being the result of some unexpected association.

## **Geological background**

The Au-Cu Palai-Islica is hosted by andesites/dacites of the Cabo de Gata-Cartagena volcanic belt (Fig. 1) which comprises part of the eastern end of the Internal Zone of the Betic Cordillera. This magmatism occurred during extensional collapse of the Betic-Alboran Domain during the Miocene, concomitant with N-S to NW-SE convergence of the Africa and Iberian plates (e.g. DEWEY 1988, GARCÍA DUEÑAS et al. 1992, LÓPEZ RUIZ & RODRIGUEZ BADIOLA 1980, FERNÁNDEZ SOLER 1996, TURNER et al. 1999). Different series of volcanic rocks developed: calc-alkaline, shoshonitic, potassic calc-alkaline, ultrapotassic and basaltic series (Fig. 1a; LÓPEZ RUIZ & RODRIGUEZ BADIOLA 1980). Magmatism extrusion was favoured by regional strike-slip fault systems which (HERNANDEZ et al. 1987), being the calc-

alkaline rocks the most abundant products. They appear in the Cabo de Gata region (LÓPEZ RUIZ & RODRIGUEZ BADIOLA 1980), and more abundantly underneath Alborán Sea (COMAS et al. 1999, FERNÁNDEZ-SOLER & COMAS 2001). Associated hydrothermal systems controlled by systems of faults and fractures originated precious and base metals deposits, being gold bearing deposits concentrated in the calc-alkaline rocks. From south to north: Cabo de Gata (PINEDA VELASCO 1984), Rodalquilar (e.g. ARRIBAS et al. 1995) and Palai-Islica (e.g. MORALES-RUANO et al. 2000; CARRILLO-ROSÚA et al. 2003a), being the last scope of this study. The Palai-Islica deposit, located ~3 Km north-east from the Carboneras town (Fig. 1b), outcrops as a kilometric size area of pervasive hydrothermal alteration over andesites/dacites. These vulcanites, of 10 Ma on age (BELLON et al. 1983), correspond to porphyritic breccias and auto-breccias. The deposit is limited to the west by the Carboneras Fault Zone (e.g. KELLER 1995), which put in contact the hydrothermally volcanic rocks with the metamorphic basement (Fig. 1b).

## **Samples and analytical technichs**

Two hundred and twenty-two polished thin-sections, from high-grade gold (up to 21 gram/tom) to barren mineralization, collected from 21 drill cores, were prepared to determine the mineralogy, the paragenetic relationships and the mineral chemistry in the Palai-Islica deposit.

Sphalerite crystals were characterized by transmitted and reflected light microscopy, scanning electron microscopy (ZEISS DSM 950 and LEO GEMINI) and Electron Probe Microanalyzer (CAMECA SX-50) of the “Centro de Instrumentación Científica” from the University of Granada. Backscattered and X-ray images were obtained to detect chemical zonations. The operating conditions for the X-ray mapping were 30 kV accelerating potential, 200 nA beam current, 2 $\mu$ m scan distance, and 0.3 seconds X-ray peak acquisition time per

point. A total of 210 EPMA analyses of sphalerite were obtained with the following operating conditions: 30 kV accelerating potential, 30 nA beam current, and between 60 (for Zn) and 440 (for In) seconds X-ray peak and background acquisition times. Natural and synthetic-certified standards were used to calibrate quantitative analyses, being corrected the acquired X-ray intensities by the CAMECA-PAP version of the POUCHOU & PICOIR (1984) procedure.

## **Mineralisation**

The Palai-Islica deposit consists in a system of veins and veinlets, steeply dipping, rich in precious and base metals (Fig. 2). A minor proportion of the deposit is formed by a dissemination of a gold rich, base metal-poor, assemblage in fully silicified volcanic rocks at the top of the deposit. Volcanic rocks which host the veins have a pervasive hydrothermal alteration and, in occasions, bear appreciable amounts of disseminated sulphides. MORALES-RUANO et al. (2000) found, in relation with the veins, two main horizons of geochemical anomalies (Upper Geochemical Anomaly (UGA) and Lower Geochemical Anomaly (LGA), with Au, Ag, Zn, Pb, Cd, As and Sb, being the former the most important) which contains microscopic gold grains and fluid inclusion in quartz with distinct microthermometric properties. That is, a wide variation in salinity ( $\geq 20$  wt. % eq. NaCl) over a narrow temperature range ( $\sim 250 - 300^\circ\text{C}$ ). While in the rest of the deposit, Th mainly ranges between 150 and  $300^\circ\text{C}$ , but salinity is below 10 wt. % eq. NaCl. The veins contain abundant pyrite with subordinate amounts of chalcopyrite, sphalerite and galena. Accessory ore phases are very diverse (Au-Ag alloys, different Ag-bearing sulphides and sulphosalts..., CARRILLO-ROSÚA et al. 2002, 2003b) being four the mineral association distinguished mainly in function of the predominant phases (Table 1): (A) pyrite; (B) pyrite + chalcopyrite; (C): pyrite + sphalerite + galena (+chalcopyrite); (D): pyrite (+ marcasite + sphalerite + galena + chalcopyrite). In addition, others specific mineral associations have been found in the

silicification (E: pyrite) and in the hydrothermal alteration from the accessed deepest part of the deposit (F: pyrite + chalcopyrite + bornite). Quartz, white mica (“sericite”), and chlorite with variable amounts of barite, gypsum, dolomite and siderite are the main gangue phases (CARRILLO-ROSÚA et al. 2003b). Two main stages are considered in the ore formation: 1) A pyritic stage, when a great amount of pyrite and minor base metal bearing sulphides crystallized. 2) A base metal-stage, when the majority of sphalerite, chalcopyrite and galena precipitated. Native gold and electrum with descending Au/Ag ratio precipitated at the end of pyritic stage and beginning of base metal stage (CARRILLO-ROSÚA et al. 2002).

### **Textural and chemical features of the sphalerite**

Three types of sphalerite have been distinguished according to its location: a) as inclusion in Fe-sulphides inside the veins (Fig. 3a); b) as disseminated crystals or crustiform bands in the veins (Fig. 2); c) as disseminated crystals in the hydrothermally altered volcanic rocks (Fig. 3b).

Small crystals of colourless or “light” coloured sphalerite (yellow to reddish under transmitted light microscope) are variably frequent as inclusions within pyrite in A, B and C mineral associations (Fig. 3a). In addition, tiny rounded and usually collomorphic sphalerite also appears included in marcasite and collomorphic pyrite in D mineral association.

Coarse disseminated sphalerite, and crustiform bands of sphalerite in quartz veins, postdates pyrite aggregates, in C mineral association (Fig. 2a). The petrographic study shows there are two varieties: “dark” red and another “light” coloured (from colourless, yellow and reddish, Fig. 3c & d). “Dark” red sphalerite is banded, with a complex concentric zonation (Fig. 3e). It has been found in the upper geochemical anomaly horizon only, accompanying visible gold. “Light” sphalerite is more abundant and spread, and overgrowths or replace “dark” sphalerite. Changes in colour of “light” sphalerite are also common, with a banded or

irregular zonation patterns (Fig. 3c & d). Transition between “light” and “dark” sphalerite is usually sharp, provably reflecting a dissolution limit (Fig. 3c). Rarely is gradual, with the occurrence of sphalerite with optical “transitional” characteristics.

Sphalerite is very rare in the hydrothermal alteration, with the exception of the deepest part of the deposit (mineral association type F), where it is colourless and the only type of sphalerite that shows cathodoluminescence (Fig. 3f).

The different types of sphalerite, especially such included in pyrite (Fig. 3g), in occasions host chalcopyrite inclusions (chalcopyrite “disease”) with diverse characteristics. These inclusions range from above the micron down to almost submicroscopic in size (“dusty chalcopyrite”, according to BARTON & BETHKE (1987)). The dusty chalcopyrite, which could produce an anisotropic appearance to the sphalerite under reflected light, is common in sphalerite from the vein system, especially at the limit between “light” and “dark” sphalerite (Fig. 3h). The morphology of chalcopyrite inclusions is generally irregular, sub-rounded or lamellar. Occasionally also appears “watermelon” textures with gradation in grain size.

### **Chemical features of the sphalerite**

The summary of EPMA analyses of sphalerite are shown in table 2, being relevant a significant chemical variability: Fe (0.07 – 8.66 at. %), Cu (0.00 - 1.34 at. %), Sb (0.00 – 0.67 at. %), Ge (0.00 - 0.24 at. %), Cd (0.00 - 0.24 at. %), Sn (0.00 - 0.21 at. %), In (0.00 - 0.18 at. %), Mn (0.00 - 0.15 at. %) and Ga (0.00 - 0.12 at. %). Table 2 also shows composition of sphalerite with dense chalcopyrite “disease” inclusions. There are appreciable differences in relation to Fe (Fig. 4) and other minor elements contents between different types of sphalerite.

*Sphalerite included in Fe-sulphides.* It has a relatively low Fe (0.42 – 4.75 at %) and Cd (up to 0.12 at %) and high Cu content (0.00 - 0.93 at %, average 0.31 at %), maybe related in part with under-surface chalcopyrite inclusions (due the small size of this sphalerite, not

always are transparent for microscopic examination). Sporadically high Sb values have been detected (up to 0.33 at %). It is noteworthy the Ga (up to 0.12 at %) and Ge (up to 0.29 at %) contents of sphalerite included in marcasite or collomorphic pyrite from D mineral association, much higher than in other types of sphalerite. Ga and Ge correlates positively (Fig. 5a), with an approximately Ga/Ge ratio of 1Ga:2Ge. In this Ga+Ge bearing sphalerite, in which both elements positively correlates with Cu in a 1Ga+Ge:1Cu ratio, is very low the Cd+In content (Fig. 5b).

Disseminated or crustiform sphalerite bands in the veins. The two optically distinguished varieties (and the occasional “transitional” type between both) have notable chemical differences, mainly in the Fe (Fig. 4) but also in other element contents (Table 3). “Dark” sphalerite has higher Fe (3.16 - 8.66 at. %) and Mn (0.02 - 0.13 at. %), and lower Sb (0.00 – 0.16 at. %) contents, in relation to “light” sphalerite (0.07 - 2.19 at. % and 0.00 - 0.08 at. % respectively). “Transitional” sphalerite has an intermediate composition between both (Fe: 1.97 - 4.64 at. %, Mn: 0.01 – 0.04 at. % respectively). Cd range content is similar in both types of sphalerite, but in “dark” sphalerite Cd roughly correlates with Fe content (Fig. 5c). The Sb, Sn and In contents are also significant (Fig. 6, 7). Sb, with values between 0.00 and 0.67 at. %, appears almost exclusively in “light” sphalerite, with Fe content below 1 at. %. It shows a very good positive correlation with Cu, with a Sb/Cu ratio of 0.5. Sb(+Cu) enrichments has been found related to the reddish areas within “light” sphalerite (Fig. 7a). Sn is occasionally detected in “light” and “dark” sphalerite in amounts up to 0.31 at. %. It is also associated to Cu (Fig. 6b), being 0.5 the Sn/Cu ratio. Although correlation line between Sn and Cu would cut the Sn axis in a value 0.10 at. % of Cu. In figure 7, it has observed that the Sn(+Cu) rich zones have a fine banding distribution. Finally, some appreciable In values (up to 0.20 at. %) have been found in “light” sphalerite, also with a positive correlation in respect to Cu content, although worse than in the cases of Sb and Sn (Fig. 6c).

Disseminated sphalerite in the hydrothermally altered volcanic rocks. Sphalerite has a low Fe (< 1 at. %) and Cd (< 0.13 at. %) contents, being very low the concentration of other elements. Nevertheless, it is also low the number of performed analyses.

Sphalerite + chalcopyrite “disease”. It has a Fe content lower than 4 at. % (after subtracting a Fe content equivalent to the Cu content). In occasions also has high Sn (up to 0.77 at. %) and In (up to 0.44 at. %) contents.

It has been observed there is some relation between chemistry of sphalerite and depth distribution. Thus, Fe, Cu, Sb, Mn, Ga+Ge and Sn reach the highest concentration in relation with upper geochemical anomaly horizon. By the contrary, higher values of In are reached with the increasing of depth. The same is observed for the minimum values of Cd: i.e. they increase with depth (Fig. 8).

## **Discussion**

### **Evolution of Fe content in sphalerite, the $f_{S_2}$ of ore-fluids, and their genetic implications**

Sphalerite is a common phase in the Palai-Islica deposit. It is concentrated in the veins, being very scarce in the hydrothermal alteration (with the exception of the deepest part of the deposit). This shows that Zn is incorporated by the hydrothermal fluids, and the contribution of this element from the altered rocks in the deposit is smaller. Furthermore, sphalerite is restricted to a certain event during the mineralization process. Thus, it precipitated mainly during the base-metal stage, and the amount produced during the earlier pyrite stage is smaller.

According to the paragenetic sequence and mineral chemistry of sphalerite, it is possible to establish an evolution of the Fe content in sphalerite and a subsequent evolution of  $f_{S_2}$  (SCOTT 1974) in the hydrothermal ore-bearing fluids. A first ore-stage corresponds to pyrite

precipitation, in which small amounts of sphalerite (as inclusions in pyrite) are also precipitated, characterized by a relatively low Fe content (up to 4.75 at. %). A second, base-metal bearing stage began with “dark” sphalerite precipitation, with Fe content between 3.16 and 8.66 at. %. This is related to a drop in the  $f_{S_2}$  with respect to the previous stage. The second stage continues with precipitation of “light” sphalerite, poor in Fe (between 0.17 and 2.19 at. %), which represents an increase in the  $f_{S_2}$ , reaching similar values as those prevailing during the first stage. This  $f_{S_2}$  increase could occur quickly, with a process of dissolution of previously precipitated sphalerite. Smaller oscillatory changes in  $f_{S_2}$  or temperature caused banded zonation, a typical feature during the precipitation of “dark” sphalerite at the beginning of the second ore-stage. This zonation is considered to be of primary origin. Fe diffusion has been argued for in other deposits (e.g. MIZUTA 1988, ZAW & LARGE 1996), but here is rejected as the cause of zonation.

It is noteworthy that the beginning of the precipitation of base metals such as Cu, Zn, Pb, Sb, Ag in the vein systems at Palai Islica coincides with a drop in the  $f_{S_2}$ . This  $f_{S_2}$  drop reflects the precipitation of a large amount of pyrite, mainly at the end of the pyrite stage, which, in turn, is related to the precipitation of gold encapsulated within pyrite (CARRILLO-ROSÚA et al. 2003a). Such an event could be produced by incorporation into the hydrothermal systems of other external fluids, such as magmatic brine (and also minor basinal fluids, Ga and Ge-bearing), which could contribute metals and trigger base metal sulphide precipitation. Thus, metals are mainly concentrated in the geochemical anomalies levels, where sphalerite also reaches its highest concentration in metals like Sb, Cu, Mn, Ga+Ge or Sn (Fig. 8). Fluid inclusion data and metal concentration in certain areas are compatible with a mixing process that generates a boiling phenomenon (MORALES-RUANO et al. 2000; CARRILLO-ROSÚA et al. 2003a).

## **Genetic and crystal chemistry implications of sphalerite chemistry**

Different minor elements have been detected in the sphalerite from Palai-Islica.

Cd: This element roughly correlates with Fe, but only in “dark” sphalerite, which also has a higher average Cd content. This positive correlation has been observed in sphalerite from other localities (e.g. MORE et al. 1991, PATTRICK & DORLING 1991), but not in all (e.g. WAGNER & COOK 1998). The Zn/Cd ratio has been used as a geochemical parameter (e.g. JONASSON & SANGSTER 1978, XUEXIN 1984, ZAW & LARGE 1996, GOTTESMANN & KAMPE 2007). Thus, XUEXIN (1984) argues that the highest values are found in volcano-sedimentary deposits (417 - 573) and the lowest in skarn, vein magmatic related deposits (102 – 214). In the case of Palai-Islica, it is highly variable (between 100 and 1000 +). The lowest values are found in “dark” sphalerite in the veins, while the highest are generally detected in sphalerite included in pyrite. This could support the hypothesis of a magmatic brine input related with the generation of “dark” sphalerite.

Ge and Ga: These elements are in very low concentration in the majority of sphalerite from the Palai-Islica deposit. Only sphalerite included in marcasite and collomorphic pyrite from type D mineral association has significant Ga and Ge content, in a ratio of 1Ga:2Ge. This mineral association also presents others peculiarities such as negative  $\delta^{34}\text{S}$ , a significantly lower value than that of the rest of the sulphides, which have a positive  $\delta^{34}\text{S}$  (CARRILLO-ROSÚA 2005). Ga and Ge are typical elements associated with organic matter in basin brines (e.g. MORALES-RUANO et al. 1996, MELCHER et al. 2006). Therefore, the presence of this kind of sphalerite could suggest the incorporation into the hydrothermal fluids of small amounts of fluids derived from the basin, possibly through the Carboneras fault, which shows activity around 10 Ma (KESLER et al. 1995), at approximately the time of mineralization (CARRILLO ROSÚA 2005). This could constitute quite a surprising discovery, since in gold-bearing epithermal volcanic-hosted deposits, the input into the hydrothermal

system of this kind of fluids is not considered (e.g. SIMMONS et al. 2005). Nevertheless, it has also been argued that these elements are derived from magmatic fluids during partial crystallization (BERNSTEIN 1986). In any case, the presence of this Ga-Ge bearing sphalerite and accompanying mineral association is significant since it is also related with gold horizons.

In addition, it is observed that Ga+Ge correlate positively with respect to Cu, with an approximate 1:1 ratio. JOHAN (1988) found very similar Ge values (up to 0.14 wt. %) in sphalerite from the Saint-Salvy deposit (an important Ge producing mine), which also correlates to Cu, but in a ratio of 1Ge:3Cu. We propose, as JOHAN (1988) suggested, that Ge substitutes Zn in sphalerite structure. However, in the case of Palai-Islica, this would be with different stoichiometry, and accompanied by Ga substitution:  $2\text{Ge}^{2+} + 1\text{Ga}^{3+} + 2\text{Cu}^{2+} + 1\text{Cu}^{+} \rightarrow 6\text{Zn}^{2+}$ . Furthermore, the behaviour of Ga+Ge is incompatible with Cd and In, which were also observed in the Saint-Salvy deposit by JOHAN (1988).

Sb: This is not an element which is usually detected in sphalerite in appreciable amounts (RAMDOHR 1969). Recently, BEAUDOIN (2000) described the existence of Sb-bearing acicular sphalerite (+ Cu and Ag) from the Kokanee Range, Canada, although he does not provide quantitative information. In the case of Palai-Islica, appreciable amounts of Sb in sphalerite have sometimes been found (up to 0.67 at. %), especially in “light” sphalerite in the veins, with Fe < 1%, associated with Cu, in a ratio of 1Sb:2Cu. The petrographic study rejects the notion that Sb+Cu content is related with microscopic mineral inclusions. These elements appear distributed together in certain domains which mark out a concentric zonation and perhaps twins. The incorporation of Sb+Cu could be considered a primary feature, very probably through an atomic substitution ( $\text{Sb}^{3+} + \text{Cu}^{+} + \text{Cu}^{2+} \rightarrow 3\text{Zn}^{2+}$ ), most often in certain growth planes in very Fe-poor sphalerite (and therefore conditions of relatively high  $f_{\text{S}_2}$ ). It occurred at an advanced stage of the ore evolution, during a period in which considerable

amounts of Sb (mainly in fahlores and Ag sulphosalts) precipitated from the hydrothermal fluids.

Sn: This element could form part of sphalerite in Sn-rich deposits (e.g. ONO et al. 2004). Some minor amounts of Sn (up to 0.31 at. %), also associated with Cu in a ratio of 1Sn:2Cu, are concentrated in certain growth bands in sphalerite from the veins in the Palai-Islica deposit (Fig. 7b). As in the case of Sb, an atomic substitution mechanism is proposed for its entrance into the sphalerite lattice:  $(\text{Sn}^{4+} + 2\text{Cu}^+ \rightarrow 3\text{Zn}^{2+})$ . The highest Sn contents occur mainly in “dark” sphalerite. This could reflect a higher Sn content of the hydrothermal fluids in an earlier period of the base-metal stage. Furthermore, Sn-bearing minerals such as stannite, vinciennite and collusite (CARRILLO-ROSÚA 2005), which crystallize in the pyrite stage, show a tendency of decreasing Sn content in the hydrothermal fluids from the beginning to the end of the mineralization process.

In: This element is usually associated with sphalerite in nature (e.g. JOHAN 1988, PATTRICK & DORLING 1991, ONO et al. 2004). In the Palai-Islica deposit, it appears in “light” sphalerite associated with Cu, although with a worse correlation than in the cases of Sb and Sn, and with a ratio of 1In:1Cu. This has also been documented in other sphalerite occurrences (e.g. JOHAN 1988, DI BENEDETO et al. 2005). As the paragenetic sequence shows, In concentrations increase during the late base-metal stage.

Cu: It is incorporated in Palai-Islica sphalerite in coupled substitution with Sb, Sn, Ga, Ge and In, but is also a common minor element on its own. The observed values are below the maximum Cu content in equilibrium in sphalerite (1.2 at. % at 300°C, according to KOJIMA & SUGAKI 1985).

### **The nature of chalcopyrite “disease”**

Chalcopyrite “disease” is a common feature in the Palai-Islica deposit. EPMA analyses reveal that Sn and In phases sometimes accompany chalcopyrite, perhaps corresponding to stannite ( $\text{Cu}_2\text{FeSnS}_4$ ) and roquesite ( $\text{CuInS}_2$ ). These minerals, accompanying chalcopyrite, have also been described in other hydrothermal deposits (e.g. OEN et al. 1980, KIEFT & DAMMAN 1990). The origin of chalcopyrite “disease” has been broadly discussed (e.g. BARTON & BETHKE 1987, ELDRIGE et al. 1988, KOJIMA, 1990, BORTNIKOV et al. 1991, KOJIMA 1992, BORTNIKOV et al. 1992, BENTE & DOERING, 1993, KOJIMA et al. 1995, NAGASE & KOJIMA 1997). In the case of Palai-Islica, a solid state diffusion hypothesis, (BENTE & DOERING 1993) a replacement hypothesis (ELDRIGE et al. 1988), or both, have been considered for “dusty” chalcopyrite in the “dark”-“light” sphalerite limit, as suggested by the pause in “dark” sphalerite precipitation, the corrosion textures, and the morphology of zones affected with “dusty” chalcopyrite (Fig. 3h). Hydrothermal fluids during this base-metal stage are recognized as Cu-bearing, since they produce a large amount of chalcopyrite precipitation. In the case of Fe-poor sphalerite included in pyrite, we suggest a co-precipitation process (e.g. BORTNIKOV et al. 1991). A rapid encapsulation by pyrite would avoid a replacement process or solid state diffusion process, and thus favour this hypothesis.

### **Relation between sphalerite colour, cathodoluminescence and composition**

Sphalerite colour is mainly conditioned by its Fe content, although there are other elements which could influence it (e.g. BARTON & BETHKE 1987). Thus, changes in sphalerite colouration have been observed, related with Cd or Co variation (BORTNIKOV et al. 1992, RAGER et al. 1996). In the case of Palai-Islica sphalerite, it has been deduced that there are several factors which control colour under a transmitted light microscope.

Among sphalerite in veins, two main groups of sphalerite have been distinguished: “light” sphalerite (from colourless, yellowish to reddish); and “dark” sphalerite (“dark” red to

brownish). These differ mainly in their Fe content. On occasions, there is sphalerite with transitional properties between both, and also intermediate Fe content. In addition, sphalerite from the hydrothermal alteration is colourless, and also Fe-poor. It is deduced that Fe concentrations above 3 at. % produce a “dark” red colour in sphalerite (in 30 µm thin sections), darker with increasing Fe content. Thus, “dark” sphalerite is usually banded due to small changes in colouration correlating with small variations in Fe content.

“Light” sphalerite presents marked colour changes, but not related to Fe content (Fig. 5). Nevertheless, a strong correlation is observed between Sb+Cu (and also Sn+Cu) and the yellow and light reddish colours. Uncoloured zones are free from these elements (Fig. histogram + Fig. 9). Furthermore, BEAUDOIN (2000) describes sphalerite which is rich in Sb, Cu and Ag. His illustrations are red in colour, although unfortunately quantitative values for these elements are not provided. Therefore, Sb+Cu and Sn+Cu have been demonstrated to be chromophore elements in sphalerite.

Cathodoluminescence in sphalerite is well documented in synthetic examples, but it is not a common feature in natural sphalerite (HAYWARD 1998). For instance, KUHLEMANN & ZEEH (1995) described cathodoluminescent sphalerite in Mississippi Valley-type deposits, but as far as the authors are aware, it has never been described in volcanic-hosted epithermal deposits. Cathodoluminescence in sphalerite has been related with Ag, Ti, Cu, Cd and Mn content (HAYWARD 1998), Fe being recognized as the element responsible for quenching the cathodoluminescence effect (MARFUNIN 1979). In the case of sphalerite from Palai-Islica, no apparent chemical differences have been found between cathodoluminescent and non-cathodoluminescent sphalerite. This could be attributable to trace element differences. It is remarkable that cathodoluminescent sphalerite, with perhaps some distinctive trace element content, has only been found disseminated in hydrothermally altered volcanic rocks in the deepest part of the deposit. There, this sphalerite forms a peculiar mineral association with the

other sulphides (“type F”, Table 1), different from the rest of the deposit. Therefore, the existence of cathodoluminescent sphalerite could constitute another criterion by which to recognise the existence of a “peculiar” mineralization at the base of the Palai-Islica vein system, with bornite, chalcopyrite, marcasite, enargite-stibioenargite and cathodoluminescent sphalerite, and perhaps a very shallow expression of deep “porphyry”-type mineralization.

## Conclusions

Sphalerite from the epithermal, Au-Cu volcanic-hosted, Palai-Islica deposit is mainly concentrated in the vein system during the second stage of sulphide precipitation (the so-called base-metal stage), although it appears throughout the deposit and mineralization sequence. Its composition reflects an evolution in  $f_{S_2}$  of the hydrothermal fluids, in which a drop in  $f_{S_2}$  at the end of the pyrite stage could reflect a mixing process triggering noble- and base-metal sulphide precipitation. Among these mixing fluids, sphalerite chemistry could suggest the incorporation of Ga+Ge basinal fluids.

Sphalerite has been demonstrated as bearing unequal, yet significant, amounts of minor elements, such as Cd, Ga, Ge, Sb, Sn, In and Cu, with implications as to source and evolution of ore fluids. It has been deduced that Sb, Sn and In enter into the sphalerite lattice by coupled substitution with Cu. The incorporation of Sb (up to 0.67 at. %) is significant – this element is not traditionally recognized as being associated to sphalerite. Furthermore, Sb+Cu and Sn+Cu (by  $Sb^{3+} + Cu^+ + Cu^{2+} \rightarrow 3Zn^{2+}$ ;  $Sn^{4+} + 2Cu^+ \rightarrow 3Zn^{2+}$ ) substitutions have been shown to produce red coloration in Fe-poor sphalerite. In addition, the presence of cathodoluminescent sphalerite is interesting since it could reflect distinctive trace element content, and could help to distinguish a different type of mineralization and fluid/metal source, manifested in an unexplored part of the deposit.

## Acknowledgements

This work has been supported by the Spanish projects CGL-2006-02594/BTE (Ministry of Education and Science and FEDER), and RNM-732 (Junta de Andalucía), J. Carrillo-Rosúa thanks MEC postdoctoral grant from MEC for his support. Authors are very grateful to *Fernando de la Fuente Consultores S.L.* for providing drill cores samples and for his help during field work.

## References

- ARRIBAS, A., CUNNINGHAM, C.G., RYTUBA, J.J., RYE, R.O., KELLY, W.C., PODWYSOCKI, M.H., MCKEE, E.H. & TOSDAL, R.M. (1995): Geology, geochronology, fluid inclusions, and isotope geochemistry of the Rodalquilar gold alunite deposit, Spain. - *Econ. Geol.* **90**: 795-822.
- BARTON, P.B. & BETHKE, P.M. (1987): Chalcopyrite disease in sphalerite: pathology and epidemiology. - *Am. Miner.* **72**: 451-467.
- BAWDEN, T.M., EINAUDI, M.T., BOSTICK, B.C., MEIBOM, A., WOODEN, J., NORBY, J.W., OROBONA, M.J.T., & CHAMBERLAIN, C.P. (2003): Extreme  $^{34}\text{S}$  depletions in ZnS at the Mike gold deposit, Carlin Trend, Nevada: Evidence for bacteriogenic supergene sphalerite. – *Geology* **31**: 913–916.
- BEAUDOIN, G. (2000): Acicular sphalerite enriched in Ag, Sb, and Cu embedded within color-banded sphalerite from the Kokanee Range, British Columbia, Canada. - *Can. Miner.* **38**: 1387-1398.
- BELLON, H., BORDET, P. & MONTENAT, C. (1983): Chronologie du magmatisme Néogène des Cordillères Bétiques (Espagne méridionale). – *Bull. Soc. Géol. France* **25**: 205-217.

- BENTE, K. & DOERING, T. (1993): Solid-state diffusion in sphalerites: an experimental verification of the “chalcopyrite disease”. - *Eur. J. Min.* **5**: 465-478.
- BERNSTEIN, L.R. (1986): Geology and mineralogy of the Apex germanium-gallium mine, Washington county, Utah. - *Bull. U.S. Geol. Surv.* **1577**: 9pp.
- BONEV, I.K. & KOUZMANOV, K. (2002): Fluid inclusions in sphalerite as negative crystals: A case study. - *Eur. J. Min.* **14**: 607-620.
- BORTNIKOV, N.S., GENKIN, A.D., DOBROVOLSKAYA, M.G., MURAVITSKAYA, G.N. & FILIMONOVA, A.A. (1991): The nature of chalcopyrite inclusions in sphalerite: exsolution, coprecipitation, or “disease”? - *Econ. Geol.* **86**: 1070-1082.
- BORTNIKOV, N.S., GENKIN, A.D., DOBROVOLSKAYA, M.G., MURAVITSKAYA, G.N. & FILIMONOVA, A.A. (1992): The nature of chalcopyrite inclusions in sphalerite: exsolution, coprecipitation, or “disease”?- A reply. *Econ. Geol.* **87**: 1192-1193.
- CARRILLO ROSÚA, F.J. (2005): El depósito epitermal de oro-cobre Palai-Islica (Carboneras, Almería). Mineralogía, geoquímica y metalogenia. - PhD thesis, Univ. Granada, Spain.
- CARRILLO-ROSÚA F.J., MORALES-RUANO S., BOYCE A.J. & FALICK A.E. (2003a): High and intermediate sulphidation environment in the same hydrothermal deposit: the example of Au-Cu Palai-Islica deposit, Carboneras (Almería). :In: ELIOPOULOS, D.G. et al. (eds.): Mineral exploration and sustainable development: Rotterdam, Netherlands, Millpress, pp. 445-448.
- CARRILLO-ROSÚA F.J., MORALES-RUANO S. & FENOLL-HACH-ALÍ P. (2002): The three generations of gold in the Palai-Islica epithermal deposit, Southeastern Spain. - *Can. Miner.* **40**: 1465-1481.
- CARRILLO-ROSÚA F.J., MORALES-RUANO S. & FENOLL HACH-ALÍ P. (2003b): Iron sulphides at the epithermal gold-copper deposit of Palai-Islica (Almería, SE of Spain). - *Mineral. Mag.* **67**: 1059-1080.

- COMAS, M.C., PLATT, J.P., SOTO, J.I. & WATTS, A.B. (1999): The origin and history of the Alboran Basin: insights from ODP leg 161 results.- In: Proc. Oce. Drill. Pro., Sci. Res. **161**: 555-580.
- DEWEY, J.F. (1988): Extensional collapse of orogens. - Tectonics **7**: 1123-1140.
- DI BENEDETTO, F., BERNARDINI, G.P., COSTAGLIOLA, P., PLANT, D. & VAUGHAN, D.J. (2005): Compositional zoning in sphalerite crystals. - Am. Miner. **90**: 1384-1392.
- ELDRIGE, C.S., BOURCIER, W.L., OHMOTO, H. & BARNES, H.L. (1988): Hydrothermal inoculation and incubation the chalcopyrite disease in sphalerite. - Econ. Geol. **83**: 978-989.
- FERNÁNDEZ SOLER J.M. (1996): El vulcanismo calc-alcalino en el Parque Natural de Cabo de Gata-Níjar (Almería). Estudio volcanológico y petrológico. - PhD thesis, Univ. Granada, Sociedad Almeriense Historia Natural, Spain.
- FERNÁNDEZ SOLER, J.M. & COMAS, M.C. (2001): Aportaciones al estudio petrológico de las rocas volcánicas de la cuenca de Alborán. – Bol. Soc. Espa. Miner. **24**: 127-128.
- GARCÍA DUEÑAS V., BALANYA J.C. & MARTÍNEZ MARTÍNEZ J.M. (1992): Miocene extensional detachments in the outcropping basements of the northern Alboran Basin (Betics). - Geomarine Let. **12**: 88-95.
- GOTTESMANN, W. & KAMPE, A. (2006): Zn/Cd ratios in calcsilicate-hosted sphalerite ores at Tumurtijin-ovoo, Mongolia. – Chem. Erde– Geochem. doi: 10.1016/j.chemer.2007.01.002.
- GRAMMATIKOPOULOS, T.A., VALEYEV, O. & ROTH, T. (2006): Compositional variation in Hg-bearing sphalerite from the polymetallic Eskay Creek deposit, British Columbia, Canada. – Chem. Erde– Geochem. **66**: 307-314.

- HARMS, U. & HECKMANN, H. (2004): Mineralization of Neiderberg, Northwest Rhenish Scheifergebirge: + sphalerite chemistry, fluid inclusions and sulfur isotopes. – N. J. Miner. Abh. **180**: 287-327.
- HAYWARD, C.L. (1998): Cathodoluminescence of ore and gangue minerals and its application in minerals industry. – In: CABRI L.J. et. al. (eds.): Modern approaches to ore and environmental mineralogy. Mineral. Assoc. Can. Short Course **27**, 269-325.
- HERNÁNDEZ, J., DE LAROUZIÈRE, F.D., BOLZE, J. & BORDET, P. (1987): Le magmatisme néogène Bético-Rifain et couloir de décrochement trans-Alboran. Bull. - Soc. Geol. Fran. **3**: 257-256.
- INSTITUTO GEOLÓGICO Y MINERO DE ESPAÑA (1974): Mapa Geológico de España. Escala 1:50,000. Hoja 1046 (24-42): Sorbas. - Servicio de publicaciones Ministerio de Industria.
- JOAN, Z. (1988): Indium and Germanium in the structure of sphalerite: an example of coupled substitution with copper. - Miner. Petrol. **39**: 211-229.
- JONASSON, I.R. & SANGSTER, D.F. (1978): Zn/Cd ratios for sphalerites from some Canadian sulfide ore samples. – Geol. Surv. Can. **78**, 195-201.
- KELLER, J.V.A., HALL, S.H., DART, C.J. & MCCLAY, K.R. (1995): The geometry and evolution of a transpressional strike-slip system: the Carboneras fault, SE Spain. J. Geol. Soc., Lon. **152**: 339-351.
- KIEFT, K. & DAMMAN, A.H. (1990): Indium-bearing chalcopyrite and sphalerite from the Gåsborn area, west Bergslagen, central Sweden. - Mineral. Mag. **54**: 109-112.
- KOJIMA, S. (1990): A coprecipitation experiment on intimate association of sphalerite and chalcopyrite and its bearing on the genesis of Kuroko ores. – Min. Geol. **40**: 147-158.
- KOJIMA, S. (1992): The nature of chalcopyrite inclusions in sphalerite: exsolution, coprecipitation, or “disease”?- A discussion. – Econ. Geol. **87**: 1191-1192.

- KOJIMA, S. & SUGAKI, A. (1985): Phase relations in the Cu-Fe-Zn-S system between 500°C and 300°C under hydrothermal conditions. - *Econ. Geol.* **80**: 158-171.
- KOJIMA, S., NAGASE, T. & INOUE, T. (1995): A coprecipitation experiment on the chalcopyrite disease texture involving Fe-bearing sphalerite. – *J. Miner. Petrol. Econ. Geol.* **90**: 261-267.
- KUHLEMANN, J. & ZEEH, S. (1995): Sphalerite stratigraphy and trace element composition of East Alpine Pb-Zn deposits (Drau Range, Austria-Slovenia). - *Econ. Geol.* **95**: 2073-2080.
- LÓPEZ RUIZ, J. & RODRIGUEZ BADIOLA, E. (1980): La región volcánica del sureste de España. - *Estudios Geológicos* **36**: 5-63.
- MARFUNIN, A.S. (1979): Spectroscopy, luminescence, and radiation centers in minerals. – Springer, Berlin, Heidelberg, New York, 352 pp.
- MORALES-RUANO, S., TOURAY, J.C., BARBANSON, L. & FENOLL HACH-ALÍ, P. (1996): Primary cavities with incompatible fluid fillings in Ge-bearing sphalerite from Cerro Del Toro, Alpujarride (Spain). - *Econ. Geol.* **91**: 460-465.
- MIZUTA, T. (1988): Interdiffusion rate of zinc and iron in natural sphalerite. - *Econ. Geol.* **83**: 1205-1220.
- MELCHER, F., OBERTHÜR, T. & RAMMLMAIR, D. (2006): Geochemical and mineralogical distribution of germanium in the Khusib Springs Cu-Zn-Pb-Ag sulfide deposit, Otavi Mountain Land, Namibia. - *Ore Geol. Rev.* **28**: 32-56.
- MORALES-RUANO, S., CARRILLO-ROSÚA, F.J., FENOLL HACH-ALÍ, P., DE LA FUENTE CHACÓN, F. & CONTRERAS LÓPEZ, E. (2000): Epithermal Cu-Au mineralisation in the Palai-Islica deposit, Almería, Southeastern Spain, fluid inclusion evidence of mixing of fluids as guide to gold mineralisation. - *Can. Miner.* **38**: 553-566.

- MORALES-RUANO, S., TOURAY, J.C., BARBANSON, L. & FENOLL HACH-ALÍ, P. (1996): Primary cavities with incompatible fluid fillings in ge-bearing sphalerite from Cerro Del Toro, Alpujarride (Spain). - *Econ. Geol.* **91**: 460-465.
- MORE, A.P., VAUGHAN, D.J. & ASHWORTH, J.R. (1991): Banded sphalerite from the North Pennine orefield. - *Mineral. Mag.* **55**: 409-416.
- NAGASE, T. & KOJIMA, S. (1997): A SEM examination of the chalcopyrite disease texture and its genetic implications. - *Mineral. Mag.* **61**: 89-97.
- OEN, I.S., KAGER, P. & KIEFT, C. (1980): Oscillatory zoning of a discontinuous solid-solution series: sphalerite-stannite. - *Am. Miner.* **65**: 1220-1232.
- ONO, S., HIRAI, K., MATSUEDA, H. & KABASHIMA, T. (2004): Polymetallic Mineralization at the Suttsu Vein-type Deposit, Southwestern Hokkaido, Japan. – *Res. Geol.* **54**: 453-464.
- PALERO-FERNÁNDEZA, F.J. & MARTÍN-IZARD, A. (2005): Trace element contents in galena and sphalerite from ore deposits of the Alcudia Valley mineral field (Eastern Sierra Morena, Spain). *J. Geochem. Explo.* **86**: 1-25.
- PATRICK, R.A.D. & DORLING, M. (1991): The substitution of indium and copper in natural sphalerite: A study using electron microscopy. - In: PAGEL, M. & LEROY J.L. (eds.): *Source, transport and deposition of metals*. Rotterdam, Balkema, pp. 223-226.
- PINEDA VELASCO, A. (1984): Las mineralizaciones metálicas y su contexto geológico en el área volcánica Neógena del Cabo de Gata (Almería, SE de España). – *Bol. Geol. Min.* **95**: 569-592.
- POUCHOU, J.L. & PICOIR, F. (1984): Un nouveau modèle de calcul pour la microanalyse quantitative per spectrométrie de rayons X. - *La Reserche Aérospatiale*, **3**: 167-192.
- QIU, U.N. & JIANG, Y. (2007): Sphalerite  $^{40}\text{Ar}/^{39}\text{Ar}$  progressive crushing and stepwise heating techniques. - *Earth Plane. Sci. Let.* **256**: 224-232.

- RAGER, H., AMTHAUER, G., BERNROIDER, M. & SCHÜRMAN, K. (1996): Colour, crystal chemistry, and mineral association of a green sphalerite from Steinperf, Dill syncline, FRG. - *Eur. J. Min.* **8**: 1191-1198.
- RAMDOHR, P. (1969): *The ore minerals and their intergrowths*. - Pergamon Press, Oxford, U.K
- SCOTT S.D. (1974): Experimental methods in sulfide synthesis. – In: RIBBE, P.H. (ed.): *Sulfide mineralogy*. *Rev. Miner.* **1**, Washington D.C., USA, Miner. Assoc. Am. pp 1-38.
- SIMMONS S.F., WHITE N.C. & JOHN D. (2005): Geological characteristics of epithermal precious and base metal deposits. - HEDENQUIST J.W. et al. (eds.): in: *Economic Geology 100th Anniversary Volume 1905-2005*. Soc. Econ. Geol., Littleton, Colorado, USA, pp 485-522.
- TURNER S.P., PLATT J.P., GEORGE R.M.M., KELLEY S.P., PEARSON D.G. & NOWELL G.M. (1999): Magmatism associated with orogenic collapse of the Betic-Alboran domain, SE Spain. - *J. Petrol.* **40**: 1011-1036.
- VIETS, J.G., HOPKINS, R.T. & MILLER, B.M. (1992): Variations in minor and trace metals in sphalerite from Mississippi Valley-Type deposits of the Ozark Region: genetic implications. - *Econ. Geol.* **87**: 1897–1905.
- WAGNER, T. & COOK, N.J. (1998): Sphalerite remobilization during multistage hydrothermal mineralization events- examples from sidertite-Pb-Zn-Cu-Sb veins, Rheinisches Schiefergebirge, Germany. - *Miner. Petrol.* **63**: 223-241.
- XUEXIN, S. (1984): Minor elements and ore genesis of the Fankou lead-zinc deposit, China. - *Miner. Depos.* **19**: 95-104.
- ZAW, K. & LARGE, R.R. (1996): Petrology and geochemistry of sphalerite from the Cambrian VHMS deposits in the Rosebery-Hercules district, western Tasmania: implication for gold mineralisation and Devonian metamorphic processes. - *Miner. Petrol.* **57**: 97-118.

Table 1. Summary of mineral associations and ore-mineralogy of the Palai-Islica deposit.

| Min. asso. | Style                   | Major minerals  | Accessory minerals   |
|------------|-------------------------|---|--|
| A          | Veins,<br>H. alteration | Pyrite  | Scarce: chalcopyrite, galena, sphalerite, tetradymite, tenantite   |
| B          | Veins                   | Pyrite, chalcopyrite                                  | Abundant: galena, fahlore, Au-Ag alloys, Ag±Bi±Pb(±Cu), sulphosalts, Ag sulphides and sulphosalts, collusite, vinciennite                |
| C          | Veins                   | Pyrite, sphalerite, galena, (chalcopyrite)            | Abundant: fahlore, Au-Ag alloys, Ag±Bi±Pb(±Cu), sulphosalts, Ag sulphides and sulphosalts, bornite, stannite<br>Barite as gangue mineral |
| D          | Veins                   | Pyrite, (marcasite, chalcopyrite, sphalerite, galena) | Colloform pyrite, Bi±Pb sulphosalts  |
| E          | Silicification          | Pyrite  | Native gold, native copper, chalcocite, covellite  |
| F          | H. alteration (in deep) | Pyrite, chalcopyrite, bornite,                        | Marcasite, galena, sphalerite, enargite-stibioenargite   |

Table 2. Summary of analyses of sphalerite from the Palai-Islica deposit.

| weight % | Inc. in Fe sulph. (n=28) |       |       |      | In veins (n=153) |       |       |      | Hydro. alter. (n=8) |       |       |      | + ccp disease (n=21) |       |       |      |
|----------|--------------------------|-------|-------|------|------------------|-------|-------|------|---------------------|-------|-------|------|----------------------|-------|-------|------|
|          | Min                      | Max   | Ave   | S.D. | Min              | Max   | Ave   | S.D. | Min                 | Max   | Ave   | S.D. | Min                  | Max   | Ave   | S.D. |
| S        | 31.31                    | 33.34 | 32.54 | 0.49 | 29.94            | 33.22 | 32.90 | 0.53 | 32.61               | 32.95 | 32.83 | 0.10 | 32.01                | 33.91 | 32.85 | 0.42 |
| Zn       | 59.65                    | 67.24 | 63.37 | 1.83 | 54.98            | 67.59 | 63.90 | 2.94 | 62.60               | 66.29 | 65.38 | 1.11 | 47.02                | 65.44 | 58.92 | 4.35 |
| Fe       | 0.49                     | 5.47  | 2.20  | 1.23 | 0.08             | 9.92  | 2.35  | 2.79 | 0.28                | 1.12  | 0.53  | 0.26 | 0.47                 | 10.01 | 4.04  | 2.27 |
| Mn       | 0.00                     | 0.17  | 0.02  | 0.04 | 0.00             | 0.14  | 0.02  | 0.02 | 0.00                | 0.09  | 0.02  | 0.03 | 0.00                 | 0.18  | 0.04  | 0.04 |
| Cd       | 0.00                     | 0.27  | 0.10  | 0.10 | 0.00             | 0.55  | 0.24  | 0.15 | 0.02                | 0.28  | 0.12  | 0.08 | 0.00                 | 0.55  | 0.27  | 0.13 |
| In       | 0.00                     | 0.28  | 0.04  | 0.08 | 0.00             | 0.43  | 0.02  | 0.06 | 0.00                | 0.23  | 0.04  | 0.08 | 0.00                 | 1.81  | 0.19  | 0.47 |
| Ga       | 0.00                     | 0.16  | 0.06  | 0.04 | 0.00             | 0.07  | 0.03  | 0.01 | 0.02                | 0.05  | 0.03  | 0.01 | 0.00                 | 0.15  | 0.03  | 0.03 |
| Ge       | 0.00                     | 0.42  | 0.11  | 0.11 | 0.00             | 0.08  | 0.03  | 0.02 | 0.01                | 0.04  | 0.03  | 0.01 | 0.00                 | 0.05  | 0.02  | 0.01 |
| Cu       | 0.00                     | 1.21  | 0.40  | 0.33 | 0.00             | 1.72  | 0.17  | 0.27 | 0.00                | 1.18  | 0.21  | 0.37 | 0.27                 | 8.54  | 2.72  | 2.20 |
| Sb       | 0.00                     | 0.81  | 0.18  | 0.25 | 0.00             | 1.63  | 0.08  | 0.25 | 0.00                | 0.01  | 0.00  | 0.00 | 0.00                 | 0.33  | 0.02  | 0.07 |
| Sn       | 0.00                     | 0.14  | 0.01  | 0.03 | 0.00             | 0.75  | 0.03  | 0.09 | 0.00                | 0.00  | 0.00  | 0.00 | 0.00                 | 1.07  | 0.16  | 0.27 |
| Ni       | 0.00                     | 0.01  | 0.00  | 0.00 | 0.00             | 0.02  | 0.00  | 0.00 | 0.00                | 0.02  | 0.01  | 0.01 | 0.00                 | 0.01  | 0.00  | 0.00 |
| As       | 0.00                     | 0.00  | 0.00  | 0.00 | 0.00             | 0.15  | 0.00  | 0.03 | 0.00                | 0.00  | 0.00  | 0.00 | 0.00                 | 0.45  | 0.03  | 0.12 |
| atomic % |                          |       |       |      |                  |       |       |      |                     |       |       |      |                      |       |       |      |
| S        | 48.95                    | 50.60 | 49.85 | 0.40 | 48.82            | 50.82 | 49.98 | 0.40 | 49.96               | 50.56 | 50.20 | 0.19 | 49.14                | 50.89 | 50.02 | 0.39 |
| Zn       | 45.51                    | 49.33 | 47.63 | 1.03 | 40.96            | 50.20 | 47.64 | 2.43 | 47.35               | 49.59 | 49.04 | 0.68 | 35.01                | 49.14 | 44.01 | 3.31 |
| Fe       | 0.42                     | 4.75  | 1.94  | 1.05 | 0.07             | 8.66  | 2.03  | 2.41 | 0.25                | 0.99  | 0.46  | 0.23 | 0.42                 | 8.72  | 3.53  | 1.98 |
| Mn       | 0.00                     | 0.15  | 0.02  | 0.03 | 0.00             | 0.13  | 0.02  | 0.02 | 0.00                | 0.08  | 0.02  | 0.02 | 0.00                 | 0.16  | 0.03  | 0.04 |
| Cd       | 0.00                     | 0.12  | 0.05  | 0.04 | 0.00             | 0.24  | 0.10  | 0.06 | 0.01                | 0.13  | 0.05  | 0.04 | 0.00                 | 0.24  | 0.12  | 0.06 |
| In       | 0.00                     | 0.12  | 0.02  | 0.03 | 0.00             | 0.18  | 0.01  | 0.03 | 0.00                | 0.10  | 0.02  | 0.03 | 0.00                 | 0.77  | 0.08  | 0.20 |
| Ga       | 0.00                     | 0.12  | 0.04  | 0.03 | 0.00             | 0.05  | 0.02  | 0.01 | 0.01                | 0.04  | 0.02  | 0.01 | 0.00                 | 0.11  | 0.02  | 0.02 |
| Ge       | 0.00                     | 0.29  | 0.08  | 0.08 | 0.00             | 0.05  | 0.02  | 0.01 | 0.00                | 0.03  | 0.02  | 0.01 | 0.00                 | 0.03  | 0.01  | 0.01 |
| Cu       | 0.00                     | 0.93  | 0.31  | 0.25 | 0.00             | 1.34  | 0.13  | 0.21 | 0.00                | 0.92  | 0.16  | 0.29 | 0.21                 | 6.54  | 2.09  | 1.69 |
| Sb       | 0.00                     | 0.33  | 0.07  | 0.10 | 0.00             | 0.67  | 0.03  | 0.10 | 0.00                | 0.00  | 0.00  | 0.00 | 0.00                 | 0.13  | 0.01  | 0.03 |
| Sn       | 0.00                     | 0.06  | 0.00  | 0.01 | 0.00             | 0.31  | 0.01  | 0.04 | 0.00                | 0.00  | 0.00  | 0.00 | 0.00                 | 0.44  | 0.06  | 0.11 |
| Ni       | 0.00                     | 0.01  | 0.00  | 0.00 | 0.00             | 0.02  | 0.00  | 0.00 | 0.00                | 0.01  | 0.00  | 0.00 | 0.00                 | 0.01  | 0.00  | 0.00 |
| As       | 0.00                     | 0.00  | 0.00  | 0.00 | 0.00             | 0.10  | 0.00  | 0.02 | 0.00                | 0.00  | 0.00  | 0.00 | 0.00                 | 0.29  | 0.02  | 0.08 |

Inc. in Fe sulph.: sphalerite included in Fe sulphides; In veins: disseminated or crustiform sphalerite bands in the veins; Hydro. alter.: Disseminated sphalerite in the hydrothermally altered volcanic rocks; + ccp disease: Sphalerite with chalcopyrite disease; Min: minimum; Max: maximum; Ave: average; S.D.: standard deviation ( $1\sigma$ ).

Table 3. Summary of analyses of disseminated and crustiform sphalerite bands in the veins from the Palai-Islica deposit.

| weight % | “Dark” sphalerite (n=36) |       |       |      | “Transitional” sphalerite (n=9) |       |       |      | “Light” sphalerite (n=108) |       |       |      |
|----------|--------------------------|-------|-------|------|---------------------------------|-------|-------|------|----------------------------|-------|-------|------|
|          | Min                      | Max   | Ave   | S.D. | Min                             | Max   | Ave   | S.D. | Min                        | Max   | Ave   | S.D. |
| S        | 32.53                    | 34.22 | 33.21 | 0.53 | 32.29                           | 33.08 | 32.70 | 0.24 | 29.94                      | 33.94 | 32.81 | 0.50 |
| Zn       | 54.98                    | 62.27 | 59.17 | 1.55 | 59.74                           | 64.51 | 62.79 | 1.28 | 62.42                      | 67.59 | 65.57 | 1.00 |
| Fe       | 3.59                     | 9.92  | 7.01  | 1.34 | 2.26                            | 5.33  | 3.52  | 0.98 | 0.08                       | 2.52  | 0.70  | 0.51 |
| Mn       | 0.02                     | 0.14  | 0.04  | 0.03 | 0.01                            | 0.09  | 0.04  | 0.02 | 0.00                       | 0.04  | 0.01  | 0.01 |
| Cd       | 0.06                     | 0.55  | 0.37  | 0.14 | 0.06                            | 0.33  | 0.19  | 0.08 | 0.00                       | 0.53  | 0.20  | 0.13 |
| In       | 0.00                     | 0.04  | 0.00  | 0.01 | 0.00                            | 0.00  | 0.00  | 0.00 | 0.00                       | 0.43  | 0.03  | 0.07 |
| Ga       | 0.00                     | 0.05  | 0.02  | 0.01 | 0.01                            | 0.07  | 0.04  | 0.02 | 0.00                       | 0.07  | 0.03  | 0.01 |
| Ge       | 0.00                     | 0.07  | 0.03  | 0.01 | 0.01                            | 0.06  | 0.03  | 0.01 | 0.00                       | 0.08  | 0.03  | 0.02 |
| Cu       | 0.00                     | 0.69  | 0.14  | 0.18 | 0.00                            | 0.29  | 0.05  | 0.09 | 0.00                       | 1.72  | 0.19  | 0.30 |
| Sb       | 0.00                     | 0.39  | 0.01  | 0.06 | 0.00                            | 0.21  | 0.02  | 0.06 | 0.00                       | 1.63  | 0.10  | 0.29 |
| Sn       | 0.00                     | 0.51  | 0.04  | 0.12 | 0.00                            | 0.05  | 0.01  | 0.02 | 0.00                       | 0.75  | 0.02  | 0.08 |
| Ni       | 0.00                     | 0.01  | 0.00  | 0.00 | 0.00                            | 0.01  | 0.00  | 0.00 | 0.00                       | 0.02  | 0.00  | 0.00 |
| As       | 0.00                     | 0.01  | 0.00  | 0.00 | 0.00                            | 0.00  | 0.00  | 0.00 | 0.00                       | 0.15  | 0.01  | 0.03 |
| atomic % |                          |       |       |      |                                 |       |       |      |                            |       |       |      |
| S        | 49.30                    | 50.67 | 49.94 | 0.45 | 48.98                           | 50.82 | 49.80 | 0.52 | 48.82                      | 50.70 | 50.01 | 0.36 |
| Zn       | 40.96                    | 46.36 | 43.65 | 1.28 | 45.01                           | 48.08 | 46.90 | 0.84 | 47.15                      | 50.20 | 49.04 | 0.67 |
| Fe       | 3.16                     | 8.66  | 6.05  | 1.15 | 1.97                            | 4.64  | 3.08  | 0.86 | 0.07                       | 2.19  | 0.61  | 0.45 |
| Mn       | 0.02                     | 0.13  | 0.04  | 0.02 | 0.01                            | 0.08  | 0.04  | 0.02 | 0.00                       | 0.04  | 0.01  | 0.01 |
| Cd       | 0.03                     | 0.24  | 0.16  | 0.06 | 0.03                            | 0.15  | 0.08  | 0.03 | 0.00                       | 0.23  | 0.09  | 0.06 |
| In       | 0.00                     | 0.02  | 0.00  | 0.00 | 0.00                            | 0.00  | 0.00  | 0.00 | 0.00                       | 0.18  | 0.01  | 0.03 |
| Ga       | 0.00                     | 0.03  | 0.02  | 0.01 | 0.00                            | 0.05  | 0.03  | 0.01 | 0.00                       | 0.05  | 0.02  | 0.01 |
| Ge       | 0.00                     | 0.05  | 0.02  | 0.01 | 0.01                            | 0.04  | 0.02  | 0.01 | 0.00                       | 0.05  | 0.02  | 0.01 |
| Cu       | 0.00                     | 0.52  | 0.10  | 0.14 | 0.00                            | 0.22  | 0.04  | 0.07 | 0.00                       | 1.34  | 0.15  | 0.23 |
| Sb       | 0.00                     | 0.16  | 0.00  | 0.03 | 0.00                            | 0.08  | 0.01  | 0.03 | 0.00                       | 0.67  | 0.04  | 0.12 |
| Sn       | 0.00                     | 0.21  | 0.02  | 0.05 | 0.00                            | 0.02  | 0.00  | 0.01 | 0.00                       | 0.31  | 0.01  | 0.03 |
| Ni       | 0.00                     | 0.02  | 0.00  | 0.01 | 0.00                            | 0.01  | 0.00  | 0.00 | 0.00                       | 0.01  | 0.00  | 0.00 |
| As       | 0.00                     | 0.02  | 0.00  | 0.01 | 0.00                            | 0.00  | 0.00  | 0.00 | 0.00                       | 0.10  | 0.00  | 0.02 |

Min: minimum; Max: maximum; Ave: average; S.D.: standard deviation ( $1\sigma$ ).

# Figure 1. Carrillo et al

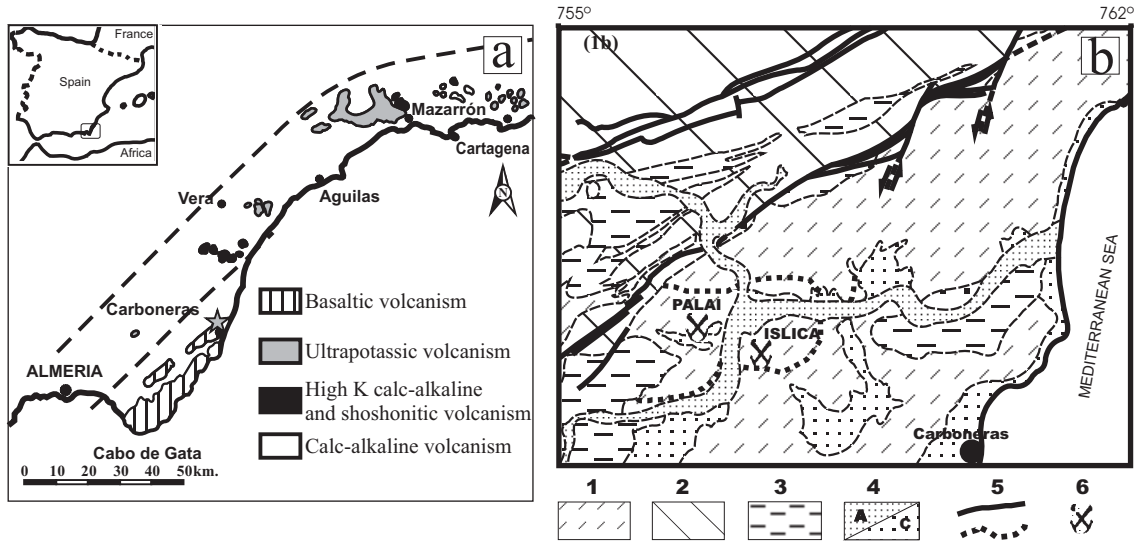


Figure 2. Carrillo et al

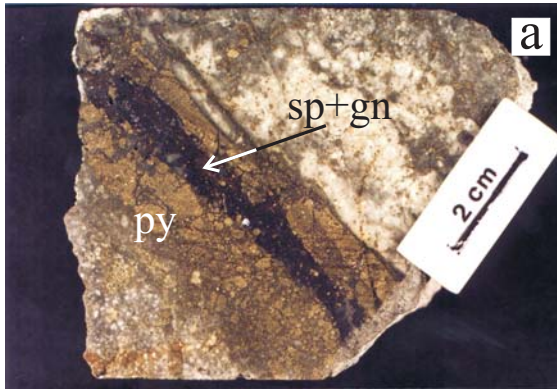
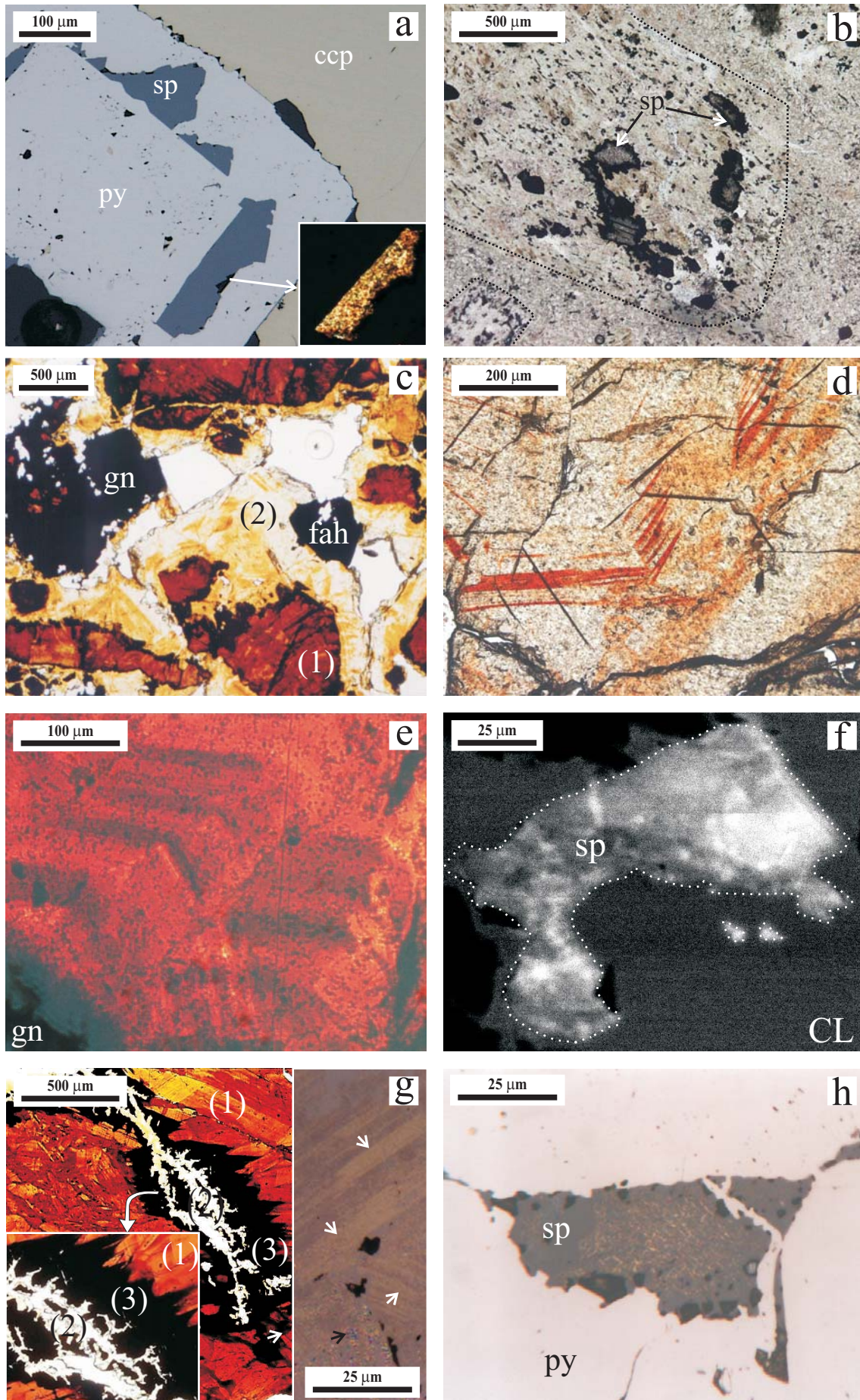
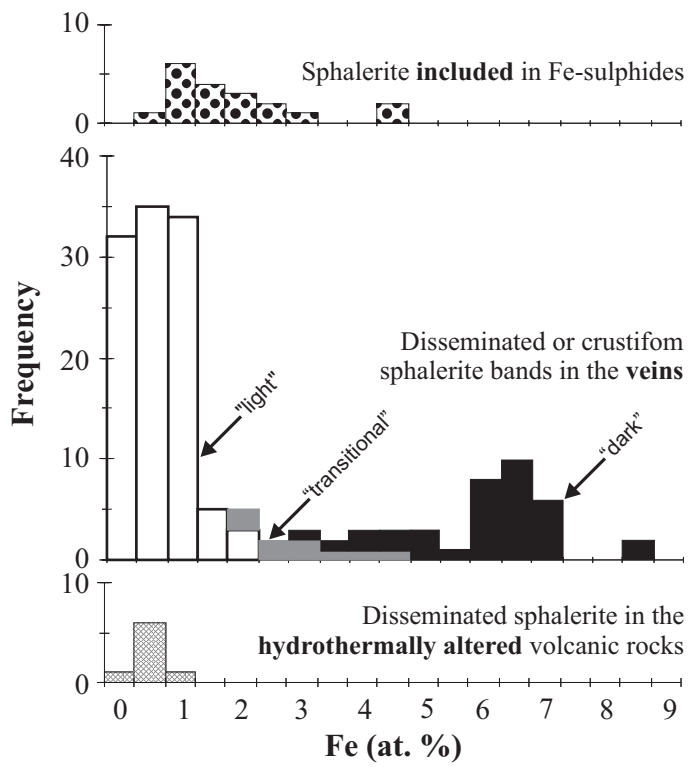


Figure 3. Carrillo et al



# Figure 4. Carrillo et al



# Figure 5. Carrillo et al

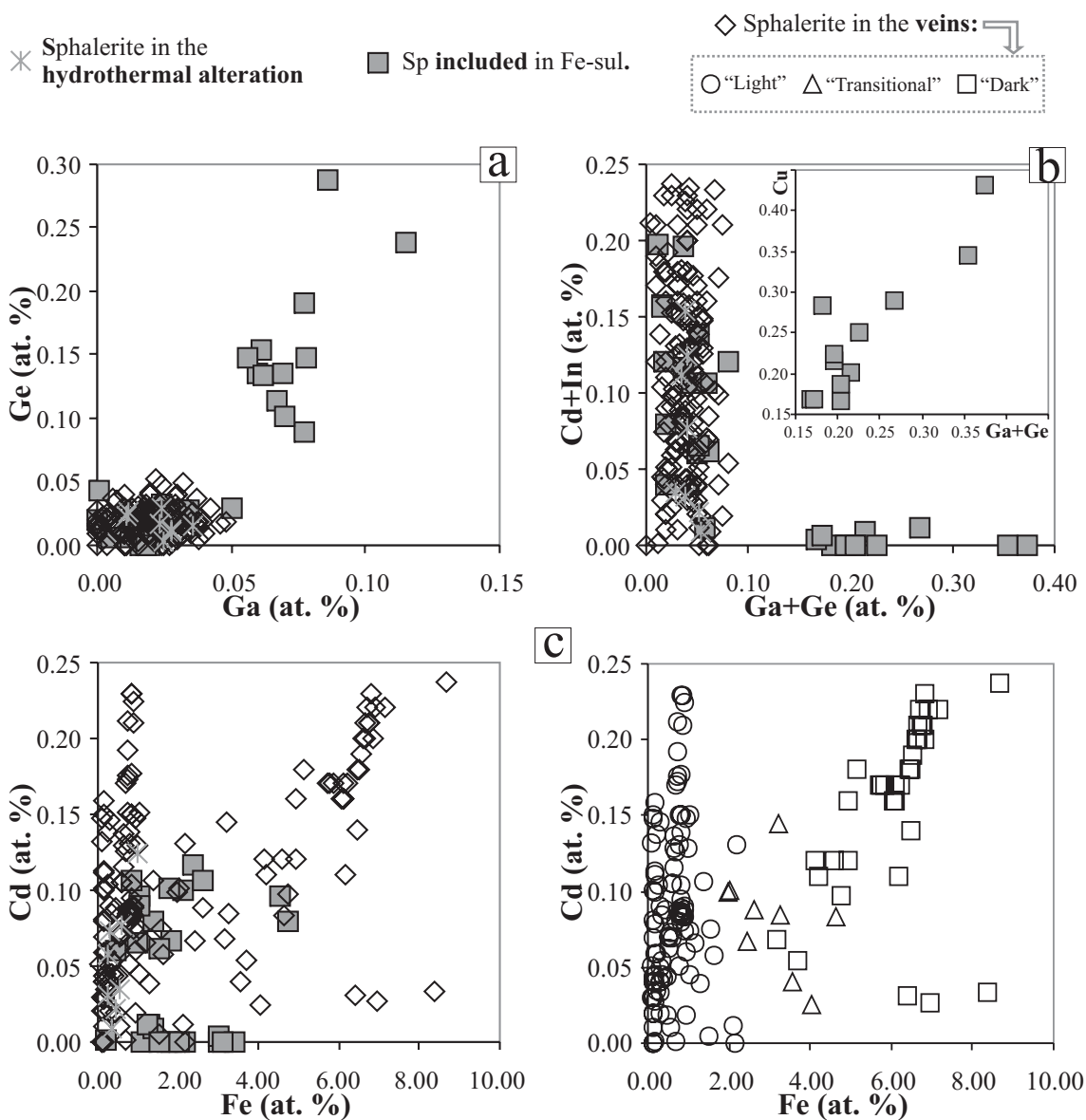


# Figure 6. Carrillo et al

○ "Light" sphalerite    □ "Dark" sphalerite  
△ "Transitional" sphalerite

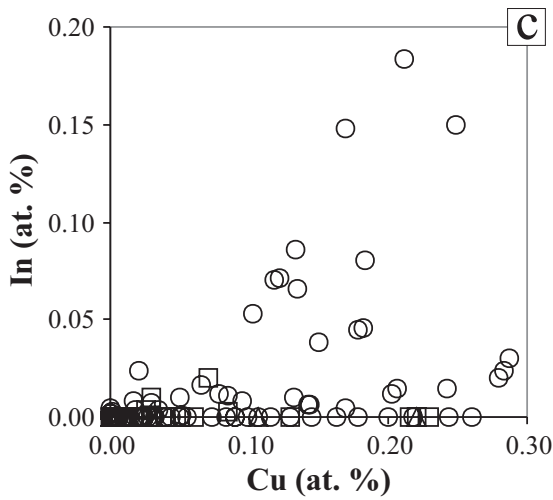
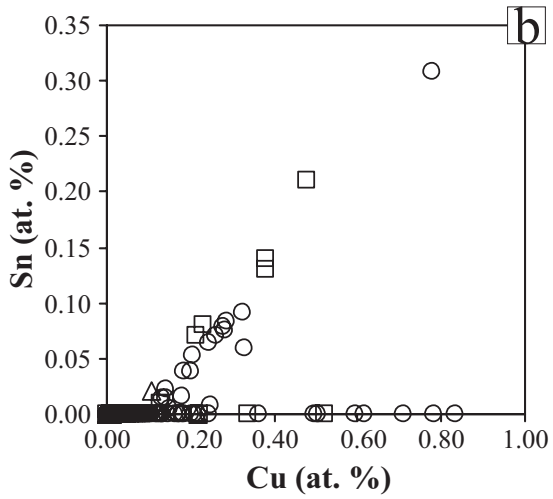
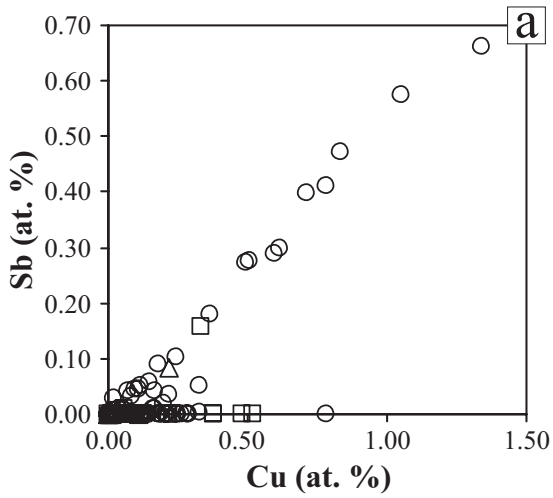
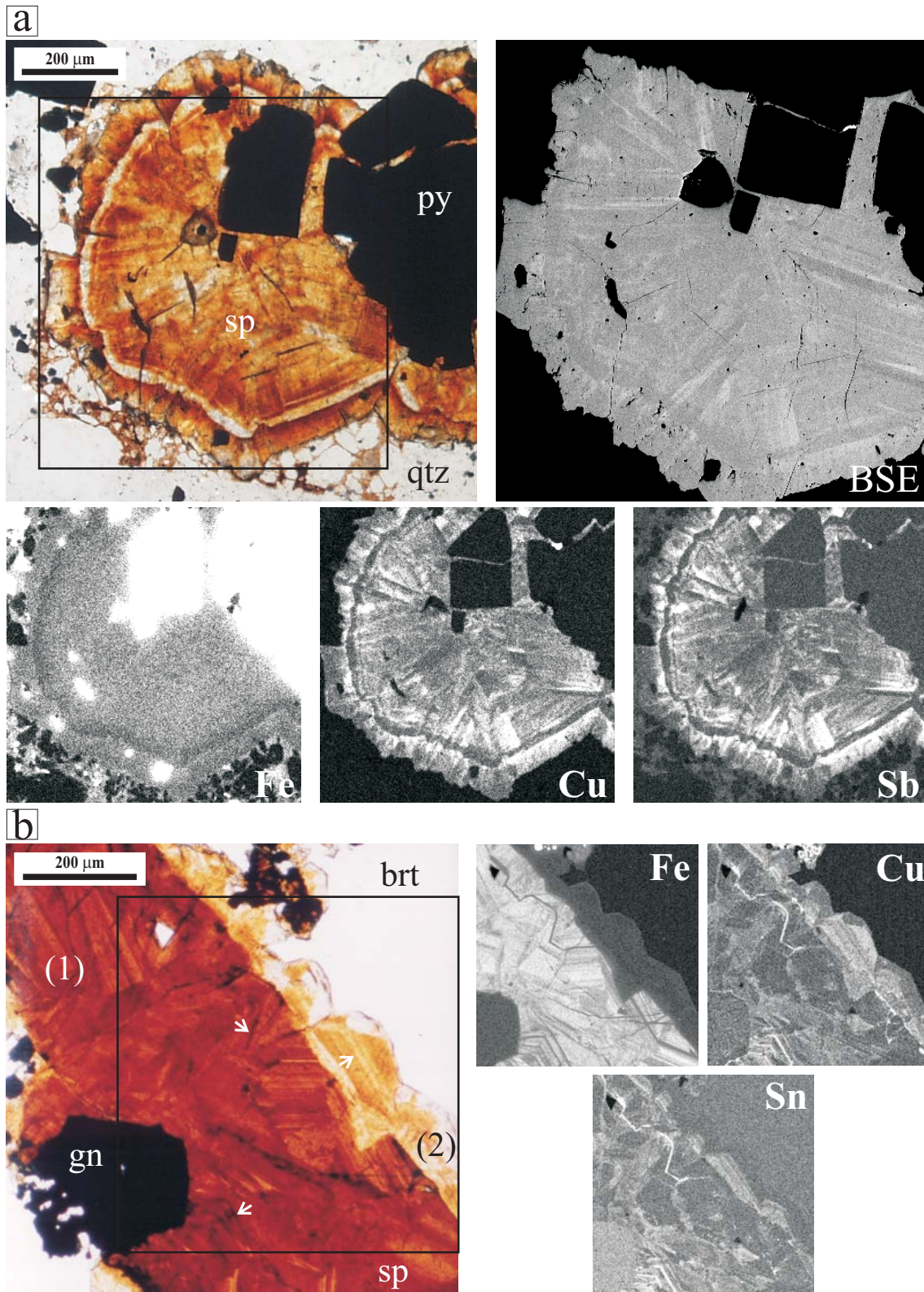
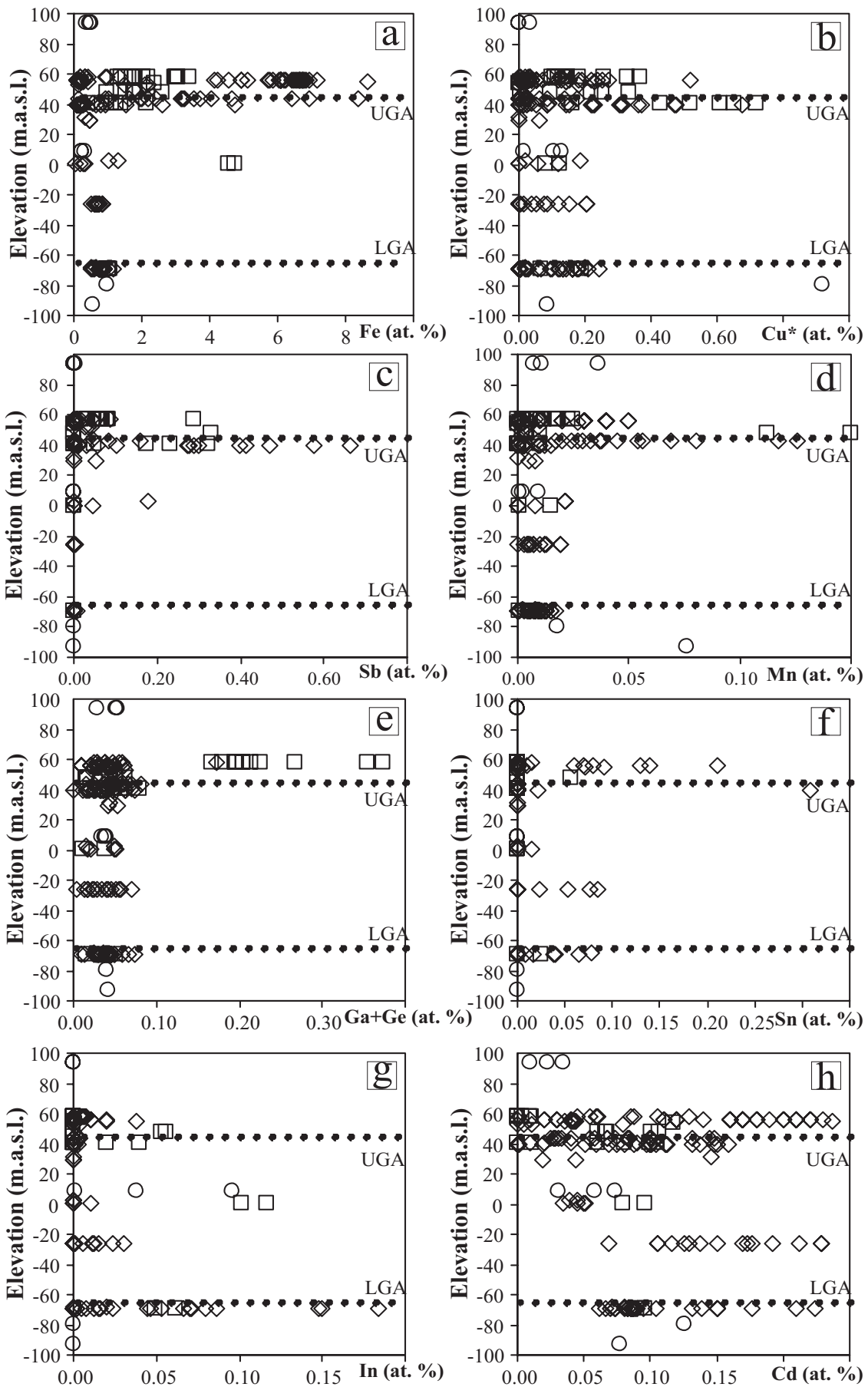


Figure 7. Carrillo et al



# Figure 8. Carrillo et al



# Figure 9. Carrillo et al

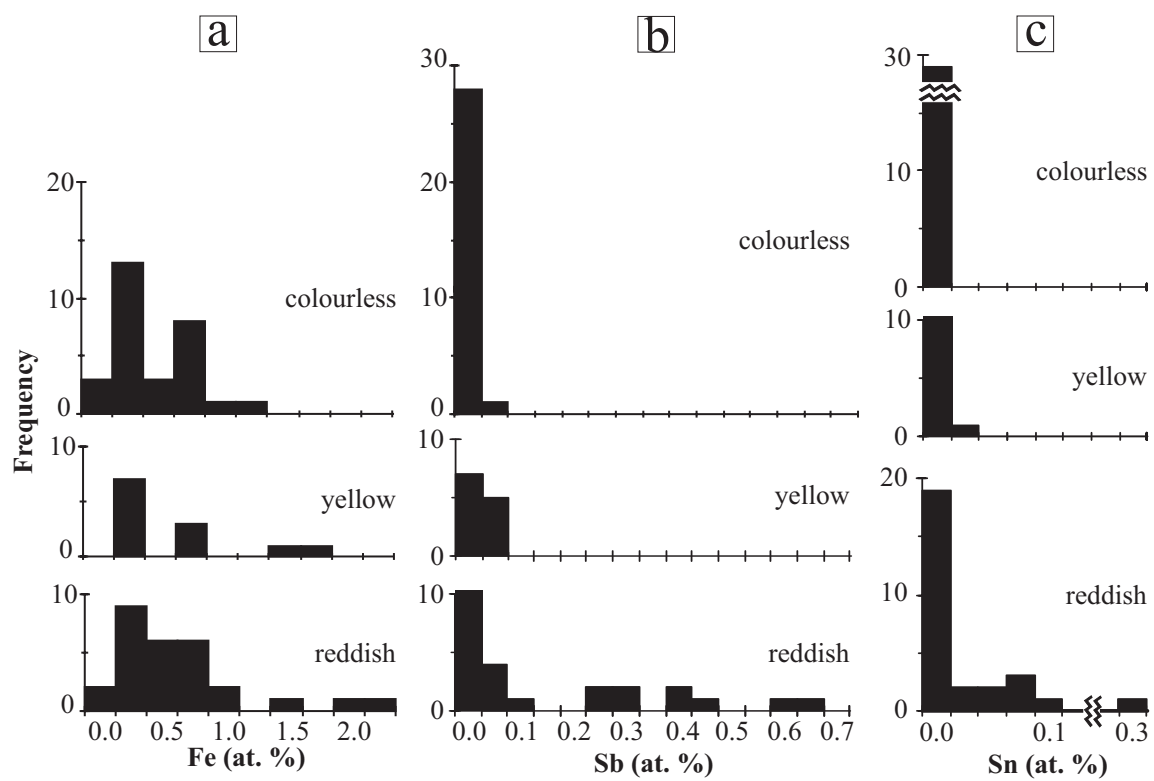


## Figure captions

### Figure 1:

(a) Cabo de Gata – Cartagena volcanic province in SE of Spain, with the Palai-Islica deposit located with a star. (b) Schematic geological map showing the location of the Palai-Islica deposit (adapted from IGME, 1974). Main geological units: (1) Upper Miocene volcanic rocks of the Cabo de Gata calc-alkaline series. (2) Paleozoic-Mesozoic basement rocks. (3) Tertiary sedimentary rocks. (4) Quaternary sediments (a) alluvial and (c) colluvial. (5) Faults are outlined in continuous line and hydrothermal alteration limit is outlined in dashed line. (6) Outcropping Palai-Islica deposit.

### Figure 2:

Hand specimens of two veins from the drill-holes, with a sphalerite-bearing mineralization (py: pyrite, sp: sphalerite; gn: galena; ccp: chalcopryrite). In (a) it is observable sl+gn is in the center of the vein, while pyrite is in margins. In (b) the veins has a brecciate character.

### Figure 3:

Reflected and transmitted light and cathodoluminescent photomicrograph of sphalerite. (a) Sphalerite included in pyrite (py). (b) Colourless sphalerite (sl) disseminated in the hydrothermal alteration, inside an transformed maphic phenocrysts (marked by a dotted line). (c) Sphalerite crystals in band within a vein. It is observed two varieties of sphalerite: one “dark” red (1) and another light colour (2), from colourless to yellow, being the limit between both sharp. (d) “Light” sphalerite in a vein with reddish bands. (e) “Dark” sphalerite with concentric zonation. (f) Cathodoluminescence in disseminated sphalerite from the type F mineral association, in the deepest part of the deposit. (g) Dusty chalcopryrite “disease” (3) in the limit between “dark” (1) and “light” (2) sphalerite. (h) Sphalerite (sp) inclusion in pyrite

(py) showing very fine lamellar and oriented chalcopyrite “disease”.

**Figure 4:**

Frequency histograms for the Fe content (in atomic percent) of the different types of sphalerite of the Palai-Islica deposit.

**Figure 5:**

Binary diagrams showing relations between minor elements (in atomic percent) in sphalerite from the Palai-Islica deposit: (a) Ga vs Ge; (b) Ga+Ge vs Cd+In and Cu; (c) Fe vs Cd.

**Figure 6:**

Binary diagrams showing relations between Sb (a), Sn (b) and In (c) and Cu (expressed as atomic percent) in sphalerite from the veins in the Palai-Islica deposit.

**Figure 7:**

Transmitted light, backscattered electron (BSE), and X-ray images of disseminated and banded sphalerite in the veins from the Palai-Islica deposit: (a) “Light” colourless, yellow and reddish sphalerite, Fe-poor, with Sb+Cu -bearing broad bands. (b) “Dark” sphalerite (1) and “light” sphalerite (2) with bands enriched in Sn+Cu (the richest ones marked with an arrow).

**Figure 8:**

Diagrams showing the relationship between chemistry (Fe, Cu\* -Cu subtracted Cu combined to Sb and Sn-, Sb, Mn, Ga+Ge, Sn, In and Cd expressed as atomic percent) of sphalerite crystals from the Palai-Islica deposit and depth (elevation in meter above sea level). Diagrams

include a dashed line indicating the position of upper (UGA) and lower (LGA) geochemical anomaly levels.

**Figure 9:**

Frequency histograms for the Fe, Sb and Sn contents of light sphalerite in the veins from the Palai-Islica deposit, according to their different colorations observed under transmitted light microscopy.

**Authors' addresses:**

J. CARRILLO-ROSÚA (e-mail: [fjcarri@ugr.es](mailto:fjcarri@ugr.es)), S. MORALES-RUANO ([smorales@ugr.es](mailto:smorales@ugr.es)) and PURIFICACIÓN FENOLL HACH-ALÍ ([pfenoll@ugr.es](mailto:pfenoll@ugr.es)).

Departamento de Mineralogía y Petrología & Instituto Andaluz de Ciencias de la Tierra, Universidad de Granada-CSIC. Avda. Fuentenueva s/n., 18002 Granada, Spain.